JACS
JOURNAL OF THE AMERICAN CHEMICAL SOCIETY
Article
pubs.acs.org/JACS

Scanning Tunneling Microscopy and Theoretical Study of Water Adsorption on Fe_3O_4: Implications for Catalysis

Kwang Taeg Rim,[†,‡] Daejin Eom,[†,‡,§] Siu-Wai Chan,[∥] Maria Flytzani-Stephanopoulos,[⊥] George W. Flynn,*[,†,‡] Xiao-Dong Wen,[#] and Enrique R. Batista[#]

[†]Department of Chemistry, Columbia University, New York, New York 10027, United States
[‡]Nanoscale Science and Engineering Center, Columbia University, New York, New York 10027, United States
[§]Department of Physics, Columbia University, New York, New York 10027, United States
[∥]Department of Applied Physics and Applied Mathematics, and Materials Research Science and Engineering Center, Columbia University, New York, New York 10027, United States
[⊥]Department of Chemical and Biological Engineering, Tufts University, Medford, Massachusetts 02155, United States
[#]Theoretical Division, Los Alamos National Laboratory, Los Alamos, New Mexico 87545, United States

Supporting Information

ABSTRACT: The reduced surface of a natural Hematite single crystal α-$Fe_2O_3(0001)$ sample has multiple surface domains with different terminations, $Fe_2O_3(0001)$, FeO(111), and $Fe_3O_4(111)$. The adsorption of water on this surface was investigated via Scanning Tunneling Microscopy (STM) and first-principle theoretical simulations. Water species are observed only on the Fe-terminated $Fe_3O_4(111)$ surface at temperatures up to 235 K. Between 235 and 245 K we observed a change in the surface species from intact water molecules and hydroxyl groups bound to the surface to only hydroxyl groups atop the surface terminating Fe^{III} cations. This indicates a low energy barrier for water dissociation on the surface of Fe_3O_4 that is supported by our theoretical computations. Our first principles simulations confirm the identity of the surface species proposed from the STM images, finding that the most stable state of a water molecule is the dissociated one (OH + H), with OH atop surface terminating Fe^{III} sites and H atop under-coordinated oxygen sites. Attempts to simulate reaction of the surface OH with coadsorbed CO fail because the only binding sites for CO are the surface Fe^{III} atoms, which are blocked by the much more strongly bound OH. In order to promote this reaction we simulated a surface decorated with gold atoms. The Au adatoms are found to cap the under-coordinated oxygen sites and dosed CO is found to bind to the Au adatom. This newly created binding site for CO not only allows for coexistence of CO and OH on the surface of Fe_3O_4 but also provides colocation between the two species. These two factors are likely promoters of catalytic activity on $Au/Fe_3O_4(111)$ surfaces.

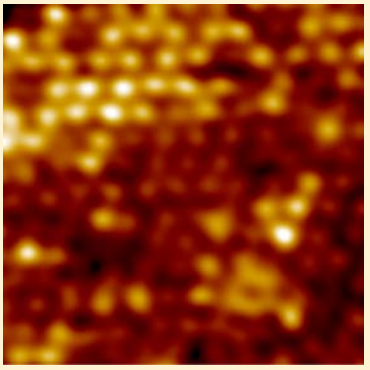

INTRODUCTION

Gold supported on metal oxide materials has recently been reported to catalyze the water gas shift reaction, an important process for the industrial production of H_2.[1−4]

$$CO + H_2O \rightarrow H_2 + CO_2$$

This observation is quite surprising since gold is normally thought of as a largely inert metal. Perhaps even more surprising is the fact that this catalytic activity remains robust even when all of the particulate gold of >1.5 nm size is removed from the oxide support, thereby indicating that the catalytically active gold represents only a small fraction of the total number of gold atoms present on the surface.[1,3] These observations naturally lead to questions about the mechanism for catalysis, particularly the importance of site-specific adsorption of Au, CO and H_2O on the metal oxide support surface.

Scanning Tunneling Microscopy (STM) studies of a gold decorated iron oxide surface, investigated in an ultrahigh vacuum (UHV) chamber, reveal the presence of single Au adatoms adsorbed at under-coordinated oxygen atom surface sites (marked by × in Figure 1a).[5] When exposed to CO, STM scans of this surface give strong indication of CO adsorption on top of the gold ad-atoms (see Figure 9 of ref 5), thereby placing adsorbed CO over oxygen atoms in the underlying iron oxide support surface.

The nature of water reactivity and adsorption on the complicated surface of natural iron oxide surfaces, which is far from completely understood, is addressed in this study both experimentally using STM and theoretically using density functional theory (DFT) calculations. Earlier computational studies of the thermochemistry of H_2O on the surface of magnetite (Fe_3O_4) provide evidence that the molecule reacts and dissociates into OH+H[6−11] but no kinetic rate information is available for this process. STM topographic images reveal the site-specific nature of adsorbed species positions on the surface,

Received: May 31, 2012
Published: October 23, 2012

 © 2012 American Chemical Society dx.doi.org/10.1021/ja305294x | J. Am. Chem. Soc. 2012, 134, 18979−18985

while Scanning Tunneling Spectroscopy (STS) conductance curves taken over individual atoms provide unambiguous differentiation of Fe and O atom sites on these surfaces. Over Fe atoms tunneling both into and out of the surface can be observed, while over O atoms only tunneling into the surface is detected in the voltage range ±2.0 V.[12,13]

Natural Iron oxide is a particularly convenient material on which to study these adsorption processes because of the previous, extensive, site-specific characterization of the material and the possibility of investigating multiple, coexisting surface terminations and phases such as those shown in Figure 1a and b, which can exist simultaneously in a single sample.[12−16] Figure 1a shows a model diagram of the top view of an Fe-terminated 2 × 2 Fe_3O_4(111) surface where the under-coordinated (uncapped) oxygen sites are marked by ×, thereby exposing both iron cations and oxygen anions to surface adsorbates[5,14] Figure 1b exhibits the top view of a purely oxygen terminated FeO(111) surface.

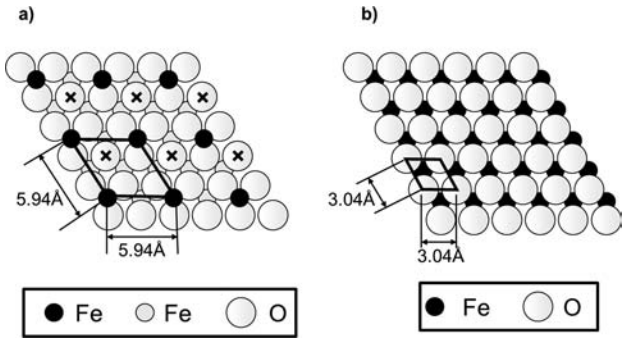

Figure 1. Top view of two possible iron oxide surface terminations. (a) Iron-terminated Fe_3O_4(111) model surface; 1/4 monolayer of tetrahedrally coordinated Fe atoms forms a 2 × 2 structure over a close packed oxygen layer, giving rise to a 5.94 Å unit cell constant. Each unit cell has an uncapped oxygen labeled by ×. (b) Oxygen-terminated FeO(111) model surface. Only oxygen atoms are exposed to surface adsorbates on this close-packed FeO(111) surface with a unit cell dimension of 3.04 Å.

In the present study we investigate the surface-termination dependent adsorption behavior of water molecules on the atomic and molecular scale at 235 and 245 K, experimentally and theoretically. STM is employed to probe the iron oxide surface with majority phase Fe-terminated 2 × 2 Fe_3O_4(111) (Figure 1a) and minority phase O-terminated FeO(111) (Figure 1b), with adsorbed water species. DFT computations are performed to determine the relative thermodynamic stability of the adsorbed water species (e.g., H_2O, OH + H) and their coexistence with Au and CO on these surfaces. These site-specific adsorption studies of water molecules on the various iron oxide surface domains are meant to pave the way for investigations into the more complex catalytic reactions involving gold decorated iron oxide surfaces.

EXPERIMENTAL AND THEORETICAL METHODS

A natural α-Fe_2O_3(0001) single crystal was cleaned in the UHV chamber by repeated cycles of Ar^+ sputtering and annealing to prepare the reduced surface film with Fe_3O_4(111) iron terminated and FeO (111) oxygen terminated domains (see Figure 1a and b), as described in detail elsewhere.[5,12−15] STM images were obtained using an ultrahigh vacuum, variable temperature scanning tunneling microscope.

The theoretical simulation results in this paper are based on plane wave expansions using the computational program VASP (Vienna Ab-initio Simulation Package).[17] The energy cutoff for the plane-wave basis was set to 500 eV. Scalar relativistic effects are included with the PAW-PBE potentials[18,19] available in the distributed code. The Brillouin zone was sampled by Monkhorst-Pack meshes of 9 × 9 × 1 for GGA+U (U_{eff} = 4.0 eV) calculations.[20] Convergence of the electronic degrees of freedom was met when the total (free) energy change and the band structure energy change between two steps were both smaller than 1×10^{-5}. We relax all structural parameters (atomic position, lattice constants) using a conjugate-gradient algorithm until the Hellmann−Feynman forces are less than 0.01 eV/Å. To investigate reaction mechanisms on a gold decorated iron oxide surface with adsorbed CO and water, the climbing image nudged elastic band (CINEB) method was performed to search transition states. The

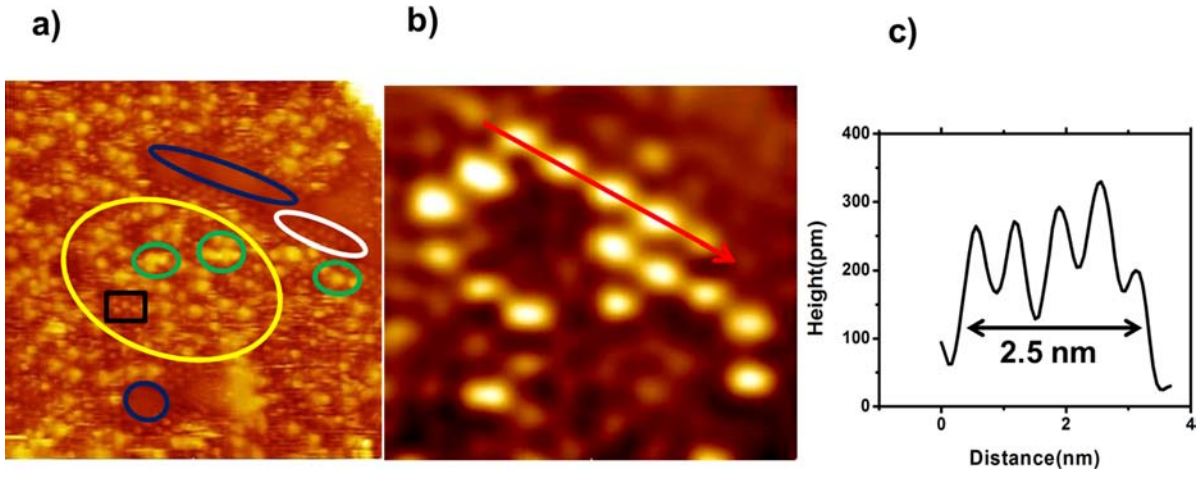

Figure 2. Topographic STM image of an iron oxide surface after dosing with water at 1.0×10^{-8} torr for 15 s at 235 K; (a) 22 nm × 22 nm, acquired at +1.3 V (sample positive) and 1.0 nA. The Fe-terminated Fe_3O_4(111) surface domain marked by the yellow oval has chemisorbed water species (small bright features marked by the black rectangle) and physisorbed water species (large circularly diffusive features marked by green ovals) on it while the O-terminated FeO(111) (blue ovals) domains do not have any adsorbed water species; (b) 5.35 nm × 4.03 nm, obtained at +1.2 V (sample positive), 1.0 nA and 235 K. The bright features atop the surface terminating Fe atoms are water-derived species. (c) Line profile along the red arrow in (b) shows that the distance (6.3 ± 0.5 Å) between these water derived adsorbates is approximately the same as that of the unit cell dimension of an iron terminated 2 × 2 Fe_3O_4(111) surface (see model for this phase in Figure 1a).

dx.doi.org/10.1021/ja305294x | J. Am. Chem. Soc. 2012, 134, 18979−18985

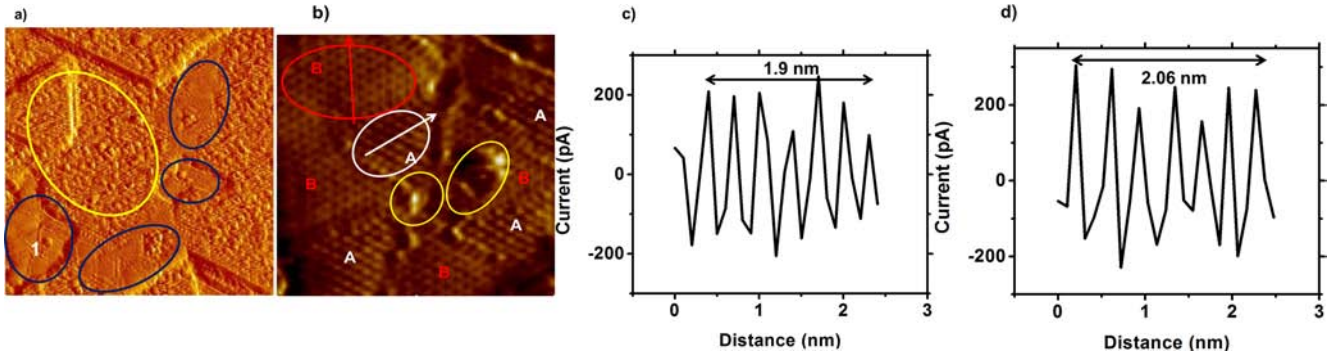

Figure 3. Constant height STM image of an iron oxide surface dosed with 0.15 L of water vapor. (a) Image (40 nm × 40 nm) recorded at 235 K (sample positive) shows an Fe-terminated $Fe_3O_4(111)$ domain marked by the yellow oval and O-terminated FeO(111) domains marked by the blue ovals. (b) Expanded image (8.12 nm × 8.12 nm) of area 1 in (a) reveals chemisorbed water species adsorbed on an Fe-terminated area marked by yellow ovals and pristine O-terminated areas (marked by A and B). (c–d) Line profiles along red (c) and white (d) arrows in (b) show distances of approximately 0.32 and 0.34 nm between atomic features, close to the unit cell distance in the oxygen layer of an unreconstructed FeO(111) surface.

reaction path was discretized with eight intermediate images between the two minima connected by elastic springs, in order to prevent the images from sliding to the minima during the course of optimization. The corresponding activation energies were calculated according to the energies between the initial and transition states.

RESULTS

Adsorption and Reaction of H_2O on the Reduced Surface of Natural Single Crystal α-Fe_2O_3. Figure 2a shows a topographic image obtained at 235 K after dosing H_2O onto the reduced surface of a natural single crystal α-$Fe_2O_3(0001)$ sample (held at 235 K) where the majority phase is a Fe-terminated 2 × 2 $Fe_3O_4(111)$ surface. The area marked by the yellow oval reveals features on this well-ordered surface with a periodicity of approximately 6 Å, which is the unit cell dimension of an Fe-terminated 2 × 2 $Fe_3O_4(111)$ surface that has exposed iron cations and oxygen anions (see Figure 1a). The ordered structure of this majority magnetite domain is readily observed in the area marked by the white oval, the boundary between the $Fe_3O_4(111)$ marked by the yellow oval, and the minority domain marked by the upper blue oval. Based on STS conductance curves, which show tunneling into but not out of these regions, the area marked by blue ovals is assigned to O-terminated FeO(111) domains that expose only closely packed surface oxygen atoms (see model in Figure 1b).

Some small bright (marked by the black rectangle) and large circularly diffusive features (marked by green ovals) are evident in the Fe_3O_4 domain marked by the yellow oval, but these only became visible after the sample was exposed to 0.15 L of water at 235 K. The diffuse features are assigned to mobile H_2O molecules physisorbed on the surface while the small bright features arise from chemisorbed, dissociated water species (e.g., hydroxyl groups). Additional features similar to these were not observed in the FeO areas (blue ovals). Figure 2b is a smaller scale topographic image (5.35 nm × 4.03 nm), revealing only small bright features without the large blurry ones (physisorbed water molecules) and substrate atoms in the $Fe_3O_4(111)$ region. We identify these features as hydroxyl groups arising from dissociative adsorption of water atop the surface terminating Fe cations. Figure 2c is a line profile along the red arrow in Figure 2b, confirming that the distance between dissociatively adsorbed hydroxyl groups (bright features) is the same as that between surface terminating Fe cations in the $Fe_3O_4(111)$ domain. The absence of water in the FeO region is consistent with temperature programmed desorption (TPD) investigations of the same system. Weiss and co-workers[21−24] reported that water species with a peak desorption temperature of 170 K are only physisorbed on the purely oxygen-terminated, ordered, epitaxial FeO(111) film grown on Pt(111).

The surface characteristics and reaction properties of O-terminated FeO(111) areas (similar to the ones marked by blue ovals in Figure 2a) and of Fe-terminated $Fe_3O_4(111)$ areas are further investigated using constant-height STM images (Figure 3), as well as being confirmed by temperature-programmed desorption (TPD) experiments,[21−24] and first principles theoretical simulations (see below).

Figure 3a shows a constant height STM image (40 nm × 40 nm) obtained at 235 K after exposing the surface to 0.15 L of water. This image reveals both the majority Fe-terminated $Fe_3O_4(111)$ area marked by the yellow oval and the minority area indicated by the blue ovals, which is predominately FeO(111). Figure 3b is an expanded image of area 1 in Figure 3a, revealing different surface phases: a triangular O-terminated FeO(111) region with no adsorbates and a Fe-terminated $Fe_3O_4(111)$ area with some additional water features marked by the yellow ovals.

Figure 3c and d are line profiles along the red and white arrows in Figure 3b revealing the distances between protruding atomic features to be 3.2 ± 0.3 and 3.4 ± 0.3 Å, respectively. These distances are close to the characteristic unit cell dimension (3.04 Å) of an unreconstructed wustite, FeO(111) surface. The area in Figure 3b marked by the yellow ovals is a Fe-terminated $Fe_3O_4(111)$ domain with some water species on it, similar to that shown in Figure 2. The areas indicated as A (white oval) and B (red oval) have the same unit cell dimension (~3.3 Å) and I(V) curves, but have slightly different corrugations. The average heights of type A and type B areas are 0.42 and 0.36 nm, respectively, and thus they are both closely packed oxygen terminated FeO(111) domains with some reconstruction occurring in the course of the formation of $Fe_3O_4(111)$ and FeO(111) domains from the original α-$Fe_2O_3(0001)$ single crystal. As such, they are likely to exhibit desorption of physisorbed water at temperatures above 170 K.[24]

TPD studies of water adsorption performed on single domain, iron terminated $Fe_3O_4(111)$ thin films grown on Pt(111) showed that thermal desorption peaks appear at 282 K for the dissociatively adsorbed water species (γ species), at 210 K for physisorbed water monomers (β species), and at 170 K for ice multilayers (α species).[24] This provides strong

dx.doi.org/10.1021/ja305294x | J. Am. Chem. Soc. 2012, 134, 18979−18985

supporting evidence that the species observed in the present STM experiments at 235 K on the Fe terminated $Fe_3O_4(111)$ domains is mostly chemisorbed water with some mobile weakly bound physisorbed water species.

TPD experiments using D_2O to dose the reduced 2 × 2 $Fe_3O_4(111)$ surface from a natural α-$Fe_2O_3(0001)$ crystal sample,[14] prepared in a manner similar to that used in the current experiment, reported several desorption peaks for chemisorbed water species at 260, 300, 340, and 595 K, respectively.[14] The fact that several recombinative desorption peaks are observed in the 260−770 K temperature range is indicative of the presence of several different surface phases with different terminations and some defects. (see Figures 2a and 3a). The desorption temperature assigned to physisorbed H_2O in this TPD study (231 K) is very close to the 235 K value used in the present STM investigation. Thus, the TPD data are consistent with the possibility that mobile water molecules (assigned to the large, circular, diffuse blurry features marked by the yellow oval in Figure 2a) on the $Fe_3O_4(111)$ surface, or water molecules loosely bound to hydroxyls on the surface via hydrogen bonding, can coexist with chemisorbed hydroxyls at 235 K.

Our theoretical calculations of H_2O on the surface of Fe_3O_4 indicate that the minimum energy state is that of a dissociated (OH+H) molecule in agreement with previous studies by Grillo et al.[25] The dissociated state was found to be 0.49 eV lower in energy with respect to the intact H_2O molecule (see Figure 4). The adsorbed water molecule (β species) is found to

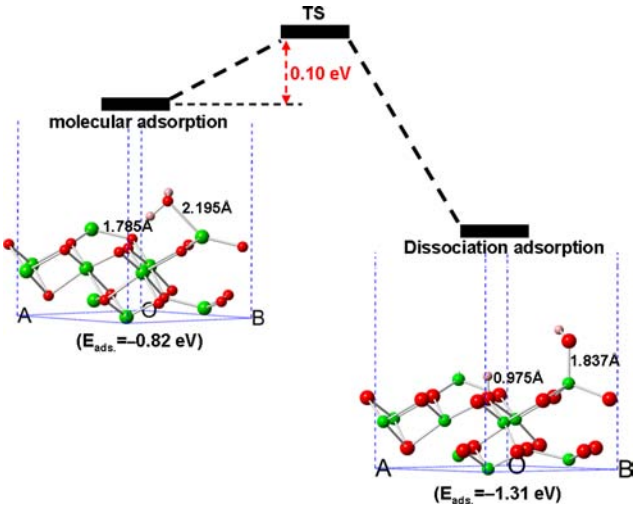

Figure 4. Optimized H_2O molecule adsorption and dissociative adsorption (OH+H), as well as the calculated minimum-energy path barrier for the dissociation process. (Red, O atoms; Green, Fe atoms; Orange, H atoms).

be weakly bound to the terminal Fe^{III} with a very long Fe−O distance of 2.2A, indicating a physisorbed species. From that state we found very small activation energy for dissociation of a water molecule (0.10 eV). The resulting OH species coordinates to the terminal Fe^{III}, as seen in the STM images (see Figure 2b), and on a clean surface the remaining hydrogen forms an OH with the under-coordinated surface oxygen atom. The OH chemisorbs on the Fe^{III} with adsorption energy of 1.31 eV, while the proton is on top of a neighboring oxygen anion resulting in single water molecule adsorption per unit cell.

Finally, if the temperature of the sample surface is raised from 235 to 245K, the topographic image changes (compare Figures 2a and 5a) indicating that the mobile water molecules, which were physisorbed on the surface at 235 K, desorbed at the higher temperature. Figure 5b, which is an enlargement of the white rectangle in Figure 5a, clearly reveals that the bright yellow features are atop the surface terminating Fe atoms, much as the hydroxyl groups identified in our DFT calculations (see Figure 4). The line profile in Figure 5c along the white arrow in Figure 5b shows the characteristic distance (~ 6 Å) between Fe atoms of a 2 × 2 $Fe_3O_4(111)$ surface. The line profile in Figure 5d along the red arrow in Figure 5b shows the same characteristic distance between bright features (hydroxyl groups). The absence of any diffuse structure in Figure 5a (comparing Figures 2a with 5a) is also consistent with desorption of mobile water molecules from the surface between 235 and 245 K.

Comparison between CO and H_2O Chemisorption. The adsorption behavior of water on different surface terminations described above and the temperature dependent behavior of these species on the complex $Fe_3O_4(111)$ surface for a given exposure is consistent with the behavior of CO adsorbed on transition metal oxides. The infrared spectroscopy of CO molecules on transition metal oxides indicates that CO is adsorbed on metal cations; thus, CO is a probe molecule for surface cations, which act as strong Lewis acid sites on these oxides, thereby attracting lone pair electrons on the water molecule.[25] The uncapped oxygen anions, on the other hand, act as Brønsted bases attracting protons from the water molecule consistent with our calculations described above.

CO molecules can be expected to adsorb atop surface terminating Fe^{III} sites of the $Fe_3O_4(111)$ surface as reported by Lemire et al on epitaxial $Fe_3O_4(111)$ films grown on a Pt(111).[26] Three adsorption states for CO were reported with desorption temperature and CO stretching frequency: the α state (~110 K, 2140−2115 cm^{-1}); the β state (~180 K, 2080 cm^{-1}); and the γ state (~230 K, 2207 cm^{-1}). This study suggests that the most strongly bound CO (230 K) is attached to Fe^{III} cations on the step edges and that the surface is terminated by 1/2 ML of iron (1/4 ML octahedral Fe^{II} and 1/4 ML tetrahedral Fe^{III} ions). The authors assigned the β and γ states to chemisorbed CO molecules attached to regular Fe^{II} sites and Fe^{III} cations along step edges, respectively.

Our DFT calculations show that CO can be physisorbed at the surface oxygen sites, while CO chemisorbs on Fe^{III} with energy of 0.46 eV, indicating that CO prefers Fe^{III} sites. Thus, there would be a competition for these Fe^{III} Lewis acid sites on a surface exposed to both CO and H_2O; however, the adsorption of dissociated water (OH) on Fe^{III} is much stronger than the adsorption of CO on these same sites.

Even though the oxidation states of surface terminating Fe cations may be mixed, depending on the preparation of the sample, it seems clear that the adsorption sites for hydroxyls after the dissociative adsorption of water are the same as those for CO molecules. TPD experiments performed as part of this CO adsorption study[26] showed that exposing the oxide surface to water blocked CO chemisorption. This is consistent with our observation that water and CO molecules compete for surface iron cation sites. Because the binding energy (1.31 eV) of hydroxyl to Fe^{III} is much stronger than that (0.46 eV) of CO, in the presence of water one would expect CO to desorb from the Fe_3O_4 surface.

dx.doi.org/10.1021/ja305294x | J. Am. Chem. Soc. 2012, 134, 18979−18985

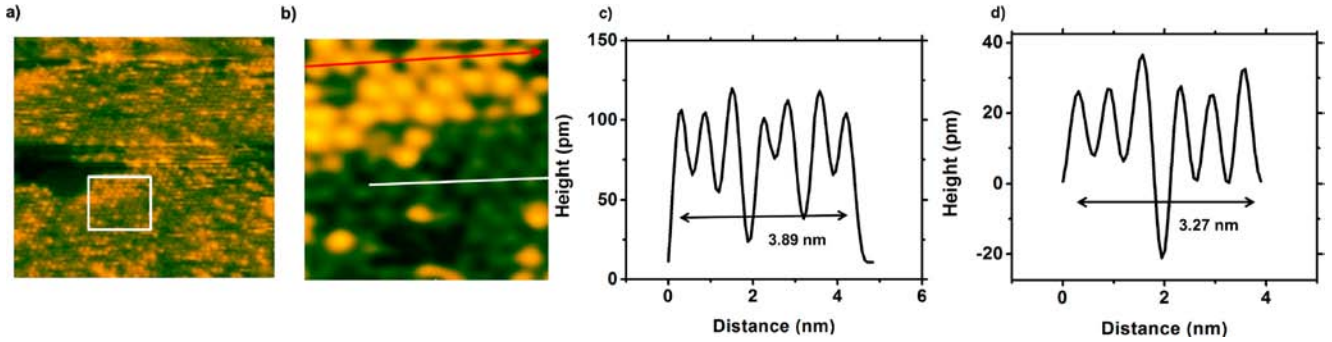

Figure 5. Topographic STM image taken at 245 K after dosing 0.1 L of water at 235 K on the iron oxide surface. (a) A 25 nm × 25 nm image at +1.0 V (sample positive) and 2.0 nA clearly shows hydroxyl groups (yellow features) on the Fe-terminated $Fe_3O_4(111)$ surface. (b) Expanded image (5.08 nm × 5.08 nm) of the area marked by the white square in (a) shows OH adsorbed atop the surface Fe atoms. (c and d) Line profiles along the white (c) and red (d) arrows in (b) show that the distance between surface irons is the same as that between OH's, confirming the location of the OH atop the surface Fe atoms.

On an iron oxide surface decorated with gold adatoms, the situation shifts quite significantly. In this case CO molecules are strongly bound to positively charged Au adatoms (which are themselves atop oxygen atoms, see Figure 9 of ref 5) rather than to surface Fe^{III} as is the case for a "pristine" $Fe_3O_4(111)$ surface.[5] Thus, CO can be expected to coexist with water on the surface of Au nanoparticle decorated iron oxide. Figure 6

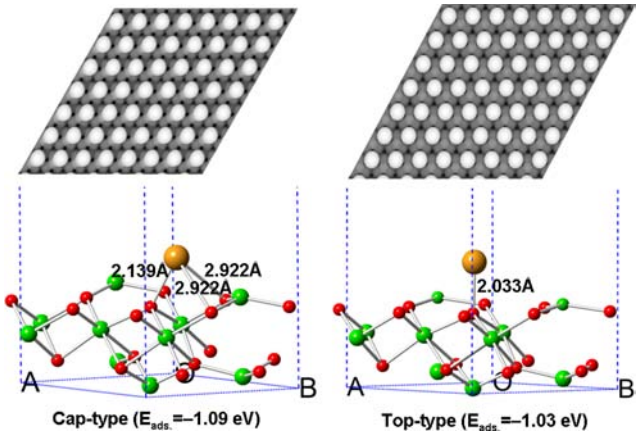

Figure 6. Two single Au adsorption configurations on $Fe_3O_4(111)$ with the corresponding STM simulated images.

shows the two most favorable adsorption sites of single Au adatoms on $Fe_3O_4(111)$. Our DFT results indicate that the most stable adsorption configuration (E_{ads} = −1.09 eV) is the cap-site type with Au sitting on the top of three O sites (two Au−O bonds at 2.922 Å and one at 2.139 Å), followed by the top-site type (−1.03 eV) Au adsorbing on one of the O atoms (Au−O, 2.033 Å). The currently computed results are in agreement with the recent study by Yu et al.[27] This small difference in energy between the two competitive adsorption structures suggests the possible mobility of Au. The simulated STM data indicate that differences between the two images would be difficult to distinguish experimentally. Note that the Au binding site is adjacent to the Fe^{III} surface atom; this colocation guarantees that any adsorbate atop gold atoms is close to any adsorbate atop Fe^{III}.

Figure 7 is a model calculated structure showing the most favorable locations for simultaneous adsorption of Au ad-atoms, CO molecules and water molecules on an iron terminated $Fe_3O_4(111)$ surface. The results of our DFT studies indicate

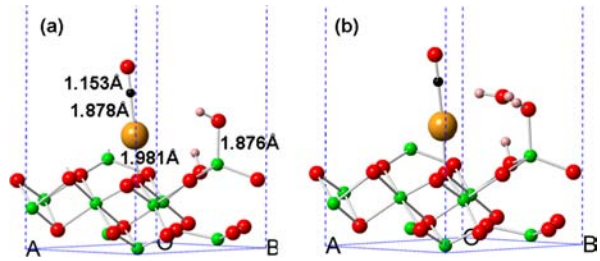

Figure 7. Coadsorption of H_2O and CO on an Au-doped $Fe_3O_4(111)$ surface. (a) Optimized H_2O dissociative adsorption on a surface with Au and CO. (b) Optimized two H_2O adsorption on a surface with Au and CO. (Red: O atoms; Green: Fe atoms; Black: C atom; Orange: Au atom; Pink: H atoms.)

that these are the most energetically favorable positions for the three adsorbates on the iron oxide surface. (See the Supporting Information for a table containing 15 more possible Au, CO, H_2O adsorption geometries and their computed adsorption energies.) The results of the calculations place the relative binding energy for adsorbates on the iron terminated $Fe_3O_4(111)$ surface in the order: Au > H_2O > CO. The Au atoms are found to coordinate to the O atom sites (marked with an × in Figure 1a), which agrees with earlier STM experimental observations.[5] For the coadsorption of Au and CO, the geometry with CO on top of Au is found to be more favorable than CO on Fe, which also agrees with the earlier STM experiments. For coadsorption of Au and H_2O, the calculations indicate that both Au and Fe are good surface sites for adsorbing H_2O. However, for the simultaneous coadsorption of Au, CO and H_2O, Fe is the favorable site for adsorption of H_2O, and Au the favorable site for CO adsorption. Thus, the adsorption of Au atoms on the iron terminated $Fe_3O_4(111)$ surface leads to an increase in the number of active sites for chemisorption, especially for CO.

We have also studied the coadsorption of H_2O and CO on an Au-doped $Fe_3O_4(111)$ surface using atomic level theoretical simulations. Figure 7a shows the optimized H_2O dissociative adsorption on an Au-doped $Fe_3O_4(111)$ surface, which is more stable by 0.25 eV than H_2O molecular adsorption on the surface. When one more H_2O is added to the surface, the H_2O forms a physisorbed adduct, as shown in Figure 7b, indicating high water mobility.

dx.doi.org/10.1021/ja305294x | J. Am. Chem. Soc. 2012, 134, 18979−18985

CONCLUSIONS

STM experiments were performed to investigate the adsorption of water on the reduced surface of a natural single crystal hematite α-Fe_2O_3(0001) sample at low temperatures. The reduced surface is composed of a majority phase domain, Fe-terminated Fe_3O_4(111), and a minority phase domain, O-terminated FeO(111). At both 235 and 245 K water was only observed on Fe-terminated regions of the Fe_3O_4(111) domain, but not on the O-terminated FeO(111) surface when the iron oxide substrate was exposed to 0.15 L of water. At 235 K, dissociated hydroxyl groups atop the surface terminating Fe^{III} sites are likely hydrogen bonded with molecular water. At 245 K, only OH groups were observed on top of Fe^{III} sites without physisorbed water molecules. Thus, the transition temperature between the hydroxylated surface and a partially dissociated water surface for a given water exposure in our ultrahigh vacuum study is approximately 240 K. These STM observations agree well with previous TPD, UPS, XPS experimental studies, as well as theoretical calculations, and provide definitive real space images of hydroxyl groups atop the iron cations.

Our theoretical studies indicate that on the surface of Fe_3O_4(111) CO and H_2O compete for the Fe^{III} binding site. Because the surface Fe^{III} facilitates the dissociation of H_2O into OH^-+H^+, the OH^- has a much stronger binding energy to the Fe^{III} than does CO. Under these conditions (only water and CO on the surface) the CO would normally desorb. The addition of Au to the Fe_3O_4(111) plays a critical role in activating the surface for CO adsorption in the presence of water. The presence of Au on the surface, bound to the under-coordinated oxygen site, provides the CO with a binding site, which is also conveniently located next to the binding site of OH. Although we do not yet have a full description of the reaction mechanism between OH and CO, this colocation plus the mobile extra water molecules that coordinate between the OH and CO, must be considered as key factors in activating any catalytic properties of the surface. Thus, in addition to any changes in the electronic structure of the iron oxide surface brought about by the adsorption of gold adatoms, the geometric arrangement of preferred surface sites for these adsorbates is likely a significant feature of any surface enhanced reactions.

Future studies will focus on water adsorption on a gold impregnated iron oxide surface and on a Au-CO prepared surface to see if these adsorbates behave differently on the more complex surfaces than on "pristine" iron oxide. STS studies of these Au/CO/H_2O decorated surfaces can also reveal how the electronic structure changes with adsorption.

ASSOCIATED CONTENT

Supporting Information

The optimized adsorption geometries and corresponding adsorption energies for each of 15 possible adsorption sites are presented in table format. For the coadsorption of Au−CO−H_2O on Fe_3O_4(111) (shown in Figure 7), we have added one more molecular H_2O coadsorbed with Au+CO, which is less stable by 0.25 eV than the geometry with the dissociated H_2O coadsorbed with Au+CO. This material is available free of charge via the Internet at http://pubs.acs.org.

AUTHOR INFORMATION

Corresponding Author

gwf1@columbia.edu

Notes

The authors declare no competing financial interest.

ACKNOWLEDGMENTS

We are indebted to Professors Jonathan Owen and Richard Osgood for stimulating discussions about iron oxide chemistry and surface structure. This work was funded by the Department of Energy under Grant Nos. DE-FG02-05ER15730 (M.F.-S., S.-W.C., and G.W.F.), DE-FG02-88ER13937 (G.W.F.), and EFRC Award DE-SC0001085 (G.W.F.). We acknowledge financial support from the New York State Office of Science, Technology, and Academic Research (NYSTAR). Equipment and material support were provided by the National Science Foundation under grants CHE-07-01483 and CHE-10-12058 (G.W.F.). Our work at Los Alamos National Laboratory was supported by the Department of Energy Heavy Element Chemistry program and the LDRD program at LANL. X.-D. Wen gratefully acknowledges a Seaborg Institute Fellowship. Some of the calculations were performed on the Chinook computing systems at the Environmental Molecular Sciences Laboratory (EMSL) at PNNL. The Los Alamos National Laboratory is operated by Los Alamos National Security, LLC, for the National Nuclear Security Administration of the U.S. Department of Energy under Contract DE-AC5206NA25396.

REFERENCES

(1) Fu, Q.; Saltsburg, H.; Flytzani-Stephanopoulos, M. *Science* **2003**, *301*, 935.
(2) Fu, Q.; Deng, W.; Saltsburg, H.; Flytzani-Stephanopoulos, M. *Appl. Catal., B* **2005**, *56*, 57.
(3) Deng, W.; Frenkel, A. I.; Si, R.; Flytzani-Stephanopoulos, M. *J. Phys. Chem. C* **2008**, *112*, 12834.
(4) Deng, W.; Carpenter, C.; Yi, N.; Flytzani-Stephanopoulos, M. *Top. Catal.* **2007**, *44*, 199.
(5) Rim, K. T.; Eom, D.; Liu, L.; Stolyarova, E.; Raitano, J. M.; Chan, S.-W.; Flytzani-Stephanopoulos, M.; Flynn, G. W. *J. Phys. Chem. C* **2009**, *113*, 10198.
(6) Grillo, M. E.; Finnis, M. W.; Ranke, W. *Phys. Rev. B* **2008**, *77*, 075407.
(7) Yang, T.; Wen, X.-D.; Huo, C.-F.; Li, Y.-W.; Wang, J.-G.; Jiao, H. *J. Phys. Chem. C* **2008**, *112*, 6372.
(8) Yang, T.; Wen, X.-D.; Li, Y.-W.; Wang, J.-G.; Jiao, H. *Surf. Sci.* **2009**, *603*, 78.
(9) Yang, T.; Wen, X.-D.; Cao, D.-B.; Li, Y.-W.; Wang, J.-G.; Huo, C.-F. *J. Fuel Chem. Tech.* **2009**, *37*, 506.
(10) Yang, T.; Wen, X.-D.; Ren, J.; Li, Y.-W.; Wang, J.-G.; Huo, C.-F. *J. Fuel Chem. Tech.* **2010**, *38*, 121.
(11) Yang, T.; Wen, X.-D.; Huo, C.-F.; Li, Y.-W.; Wang, J.-G.; Jiao, H. *J. Mol. Catal. A* **2009**, *302*, 129.
(12) Rim, K. T.; Fitts, J. P.; Müller, T.; Adib, K.; Camillone, N., III; Osgood, R. M.; Joyce, S. A.; Flynn, G. W. *Surf. Sci.* **2003**, *541*, 59.
(13) Rim, K. T.; Müller, T.; Fitts, J. P.; Adib, K.; Camillone, N., III; Osgood, R. M.; Joyce, S. A.; Flynn, G. W. *J. Phys. Chem. B* **2004**, *108*, 16753.
(14) Adib, K.; Totir, G. G.; Fitts, J. P.; Rim, K. T.; Mueller, T.; Flynn, G. W.; Joyce, S. A.; Osgood, R. M. *Surf. Sci.* **2003**, *537*, 191.
(15) Camillone, N., III; Adib, K.; Fitts, J. P.; Rim, K. T.; Flynn, G. W.; Joyce, S. A.; Osgood, R. M. *Surf. Sci.* **2002**, *511*, 267.
(16) Merte, L. R.; Peng, G.; Bechstein, R.; Rieboldt, F.; Farberow, C. A.; Grabow, L. C.; Kudernatsch, W.; Wendt, S.; Laegsgaard, E.; Mavrikakis, M.; Besenbacher, F. *Science* **2012**, *336*, 889.
(17) Kresse, G.; Hafner, J. *Phys. Rev. B* **1993**, *47*, 558.
(18) Blöchl, P. E. *Phys. Rev. B* **1994**, *50*, 17953.
(19) Kresse, G.; Joubert, D. *Phys. Rev. B* **1999**, *59*, 1758.
(20) Dudarev, S. L.; Botton, G. A.; Savrasov, S. Y.; Humphreys, C. J.; Sutton, A. P. *Phys. Rev. B* **1998**, *57*, 1505.

(21) Joseph, Y.; Kuhrs, C.; Ranke, W.; Ritter, M.; Weiss, W. *Chem. Phys. Lett.* **1999**, *314*, 195.
(22) Joseph, Y.; Kuhrs, C.; Ranke, W.; Weiss, W. *Surf. Sci.* **1999**, *433*−*435*, 114.
(23) Shaikhutdinov, S. K.; Joseph, Y.; Kuhrs, C.; Ranke, W.; Weiss, W. *Faraday Discuss.* **1999**, *114*, 363.
(24) Joseph, Y.; Ranke, W.; Weiss, W. *J. Phys. Chem. B* **2000**, *104*, 3224.
(25) Davydov, A. A. *Infrared Spectroscopy of Adsorbed Species on the Surface of Transition Metal Oxides*; John Wiley and Sons: New York, 1990.
(26) Lemire, C.; Meyer, R.; Henrich, V. E.; Shaikhutdinov, S.; Freund, H.-J. *Surf. Sci.* **2004**, *572*, 103.
(27) Yu, X.; Wang, S.; Li, Y.-W.; Wang, J.; Jiao, H. *J. Phys. Chem. C* **2012**, *116*, 10632.